Structural and elastic properties of the dipolar Gay-Berne model

A. V. Zakharov* and S. Romano[†]

*Istituto Nazionale per la Fisica della Materia, Dipartimento di Fisica ''A. Volta,'' Universitá di Pavia,
via A. Bassi 6, I-27100 Pavia, Italy*

(Received 5 June 1998)

A statistical-mechanical theory based upon the method of conditional distribution functions, and taking into account translational and orientational correlations as well as their coupling, has been applied to calculate structural and elastic properties of a system comprised of interacting cylindrically symmetric particles. Calculations have been carried out for a simple-cubic parking, and using two interaction models, i.e., both the usual Gay-Berne potential and the same model supplemented by a truncated dipolar term. An extensive study of both models over a range of temperatures and densities has provided detailed information on the elastic behavior of their resulting nematic phases. Our results also show that the elastic properties are affected in a more pronounced way by changes in the thermodynamic conditions than by the dipolar contribution in the potential. [S1063-651X(98)00212-8]

PACS number(s): 61.30.Cz, 64.70.Md

I. INTRODUCTION

The variety of mesophases formed by anisotropic molecules interacting via the Gay-Berne (GB) potential [1] has stimulated the interest of researchers. Rull and co-workers [2] described a complete diagram of the GB fluid, using the parametrization originally proposed by Gay and Berne [1], and found isotropic (I), nematic (N), and smectic B (Sm B) phases. Luckhurst's group carried out extensive simulations [3], using a different choice of potential parameters, and found that, in addition to I, N, and SmB, a SmA phase also appeared; a recent and extensive simulation study of the effect of elongation on the phases diagram can be found in Ref. [4]. Nevertheless, it should be pointed out that a number of fundamental questions still remain unanswered, even though numerous studies have been undertaken in this area. One of them concerns the influence of microscopic correlations and interactions among molecules composing the liquid-crystal phase on such measurable quantities as Frank elastic constants and viscosity [5].

Over the years, quite a few microscopic theories have been developed, both for bulk and surface elastic constants [6–8]. On the other hand, in practice, it is difficult to measure the absolute values of these elastic coefficients. For example, it has been shown [9] that the experimental results for K_{11} and K_{22} (splay and twist distortion modes, respectively) have a weak temperature dependence, whereas K_{33} (bend distortion mode) rapidly increases with temperature. However, computer simulations of the GB nematic liquid crystals show [7] that all three elastic contents have the same, nearly linear, temperature dependences.

The long-term aim of our research is a detailed understanding of the effect of dipolar contributions on structural behavior and on measurable macroscopic quantities reflecting underlying microscopic interactions and correlations. Identification of the molecular features and correlations among molecules, which compose a nematic phase, that influence its elastic behavior is thus of primary interest.

The effect of dipolar interactions on mesomorphic behavior has recently been studied by Monte Carlo simulations (MC), based on dipolar GB potentials [10–12]. In contrast to pure GB models, bulk and surface elastic constants for these models have not yet been investigated. Of course, a common intuitive notion is that the additional dipole-dipole interaction has a greater influence on molecular structure than on macroscopic quantities such as elastic constants. Nevertheless, a theory capable of estimating the effect of dipole-dipole interactions on the behavior of elastic constants would be most desirable.

In this paper, we perform calculations of order parameters and Frank bulk elastic constants K_{11}, K_{22}, and K_{33}, both for the usual GB fluid and for dipolar ones. This has been realized theoretically by combining the previous advantages [13] of integral equation approaches with microscopic expressions for the elastic constants in terms of the direct correlation function (DCF) [14,15].

The present paper is organized as follows: a description of the statistical-mechanical treatment is given in Sec. II, the numerical solution of the resulting nonlinear integral equations is discussed in Sec. III, intermolecular potentials are described in Sec. IV, statistical-mechanical expressions for the Frank constants are given in Sec. V, and numerical results are given in Sec. VI; we finally summarize our main results and conclusions in Sec. VII.

II. STATISTICAL-MECHANICAL TREATMENT

We consider here a classical one-component fluid, consisting of cylindrically symmetric particles; let $\mathbf{q}_i$ denote their center-of-mass coordinates, and let $\mathbf{e}_i$ denote unit vectors defining their orientations; in the following the collective symbol $i \equiv (\mathbf{q}_i, \mathbf{e}_i)$ will also be used. One considers N such particles occupying a volume V at the temperature T;

---

*Author to whom correspondence should be addressed. Electronic address: avz@physc.su.se Permanent address: Saint Petersburg Institute for Machine Sciences, the Russian Academy of Sciences, Saint Petersburg 199178, Russia.

[†]Electronic address: romano@pv.infn.it

one can ideally subdivide to total volume into N cells, each with volume $v = V/N$. The treatment used here further assumes that each cell is occupied by one and only one molecule. Particles are assumed to interact via a pairwise additive potential $\Phi(i,j)$, so that the total interaction energy for the N particles is $U = \Sigma_{i<j} \Phi(i,j)$. The quantity $\exp(-\beta U)$ is the canonical probability density; upon integrating out the coordintes of remaining particles, one can define single-particle probability densities $F_i(i)$, two-particle probability densities $F_{ij}(ij)$, and so on [13,16]; we truncate the infinite hierarchy at the two-particle level. By the partitioning of space mentioned above, $F_i(i)$ is the probability density for a single particle confined inside a cell of volume v, and $F_{ij}(ij)$ is a probability density for two particles confined in two different cells. The above-mentioned functions can also be written in terms of mean-force potentials (MFP's), i.e.,

$$F_i(i) = (1/Q)\exp(-\beta \varphi_i(i)), \qquad (1)$$

$$F_{ij}(ij) = (1/Q^2)\exp\{-\beta[\varphi_{ij}(ij) + \Phi(ij)]\}, \qquad (2)$$

where

$$Q = \int_i d(i)\exp(-\beta \varphi_i(i)), \quad \int_i d(i) = \int_w d\mathbf{q}_i d\mathbf{e}_i.$$

Here $\beta = \theta^{-1} = (k_B T)^{-1}$ is the inverse temperature and $w = v \otimes \alpha$, where α is the volume associated with orientations. The functions $\varphi_i(i)$ and $\varphi_{ij}(ij)$ are singlet and binary mean-force potentials, given by sums of the form

$$\varphi_i(i) = \sum_{j \neq i} \varphi_{i,j}(i), \qquad (3)$$

$$\varphi_{ij}(ij) = \sum_{l \neq i,j} \varphi_{ij,l}(ij). \qquad (4)$$

Here $\varphi_{i,j}(i)$ and $\varphi_{ij,l}(ij)$ are mean-force potentials: $\varphi_{i,j}(i)$ is the singlet mean-force potential for a molecule in the ith cell, due to a molecule in the jth cell, and averaged over the state of the latter. Similarly, $\varphi_{ij,l}(ij)$ is the binary mean-force potential of molecules i and j in the ith and jth cells, due to a molecule in the lth cell, and averaged over the state of the latter. The subscripts before the comma correspond to the MFP dependence on the coordinates of molecules; the subscript after the comma corresponds to the average states. Using now the relations between singlet and binary functions which follow from their definition, one has

$$\int_i d(i) F_i(i) = 1, \quad \int_j d(j) F_{ij}(ij) = F_i(i). \qquad (5)$$

The two-particle function is similarly related to a three-particle function by an integral relation, etc. Here and in the following we take into account only singlet- and two-particle functions of the infinite hierarchy, i.e., only pair correlations between cells. In order to obtain a closed set of equations, we separate the MFP's into irreducible parts [13,16]. To the approximation considered here, i.e., neglecting three-cell and higher-order correlations, we have

$$\varphi_{ij,l}(ij) = \varphi_{i,l}(i) + \varphi_{j,l}(j), \qquad (6)$$

and then the expressions for binary mean-force potential $\varphi_{ij}(ij)$ and function $F_{ij}(ij)$ take the forms

$$\varphi_{ij}(ij) = \varphi_i(i) + \varphi_j(j) - \varphi_{i,j}(i) - \varphi_{j,i}(j),$$

$$F_{ij}(ij) = Q^{-2}\exp\{-\beta[\Phi(ij) + \varphi_i(i) + \varphi_j(j) - \varphi_{i,j}(i) - \varphi_{j,i}(j)]\}.$$

Using now the definitions

$$\psi \equiv \exp(-\beta \varphi), \quad V(ij) = \exp(-\beta \Phi(ij)),$$

the expressions for binary functions takes the form

$$F_{ij}(ij) = F_i(i) F_j(j) V(ij) \psi_{i,j}^{-1}(i) \psi_{j,i}^{-1}(j). \qquad (7)$$

The last three factors in Eq. (7) reflect correlations betwen cells, which distinguishes the approach used here from mean-field approximations. Substitution of Eq. (7) into Eq. (5) leads to a closed system of nonlinear integral equations (NIE's) for the MFP's [13],

$$\psi_{i,j}(i) = \int_j F_j(j) V(ij) \psi_{j,i}^{-1}(j), \qquad (8)$$

where

$$F_j(j) = \frac{\psi_j(j)}{\int_j \psi_j(j) d(j)}. \qquad (9)$$

Equations (3), (8), and (9) now provide a closed system of nonlinear integral equations for the MFP's. After solving these equations, one can compute microscopic properties of a liquid-crystalline system, expressed in terms of one- and two-particle functions, as well as thermodynamic ones expressed in terms of the free energy [13,16], i.e.,

$$f = F/N = -\beta^{-1}\ln \int_i \psi_i(i) d(i), \qquad (10)$$

$$\psi_i(i) = \prod_{j \neq i} \psi_{i,j}(i). \qquad (11)$$

In Eq. (11), the $\prod_{j \neq i}$ run over all neighbors of cell i. Note that the same system of equations appears in the Bethe approximation for a lattice model of surfactant mixtures [Eq. (12) in Ref. [17], and Ref. [18]]; let us also mention that the present approach is similar in spirit to cluster variational methods, originally developed for magnetic lattice spin models (see, e.g., Ref. [19]), and later used for nematogenic lattice models as well (see, e.g., Refs. [20,21]). In Ref. [21] both the two-site cluster method and computer simulation were used to study a lattice model consisting of three-component unit vectors, associated with a simple-cubic lattice, and interacting via a nearest-neighbor potential of the form $-a P_2(\eta) + b P_1(\eta)$, $\eta = \mathbf{e}_i \cdot \mathbf{e}_j$, where $a > 0$, and the b term crudely allows for polar effects; here P_1 and P_2 denote first- and second-order Legendre polynomials.

III. METHOD OF SOLUTION FOR THE SYSTEM OF NONLINEAR INTEGRAL EQUATIONS

The problem of solving the five-dimensional problem (8) is very complicated, and there are no good general methods for more than one nonlinear equation. Except for linear problems, solutions are invariably obtained by a numerical iterative procedure, using the formula

$$\psi^{[k+1]}(P_i) = \{\psi^{[k]}(P_i)\hat{L}\psi^{[k]}(P_i)\}^{1/2}, \qquad (12)$$

where $\hat{L}, \|\hat{L}\| \leq 1$ is the five-dimensional nonlinear integral operator defined by Eq. (8) in the space $w_i = v \otimes \alpha$, and P_i is a five-dimensional vector in the same space.

The problem of the existence and uniqueness of the solution for the one-dimensional problem has been investigated by Kronrade (see Ref. [22]), and this finding can be generalized to multidimensional domains as well [23]. For smoothly varying functions, good algorithms will always converge, provided the initial guess is accurate enough; thus success strongly depends on a good initial guess for the solutions $\psi(P_i)$. The algorithm (12) was implemented as follows: the initial approximation was set to

$$\psi_{i,j}^{m[0]}(P_i) = \text{const}$$

and

$$\psi_i^{[0]}(P_i) = \prod_{m=1}^{l} \prod_{j\neq i}^{N_m} \psi_{i,j}^{m[0]}(P_i),$$

where l is the number of neighbors and N_m is their quantities.

The integrals in the right-hand side of

$$\psi_{i,j}^{m[k+1]}(P_i) = \{\psi_{i,j}^{m[k]}(P_i)\hat{L}\psi_{i,j}^{m[k]}(P_i)\}^{1/2}, \qquad (13)$$

for $m = 1,2,\ldots,l$, have to be calculated numerically, i.e.,

$$\int_0^1 dx_1 \cdots \int_0^1 dx_n f(x_1,x_2,\ldots,x_n) \approx (1/M) \sum_{\alpha=1}^{M} f(P_\alpha), \qquad (14)$$

where the points are chosen according to some suitable criterion: a straightforward Monte Carlo integration yields a precision $R \sim O(1/\sqrt{M})$, whereas Sobol's method (LP_τ sequence [24], see also the Appendix) produces $R \sim O(M^{-1}(\ln M)^n)$.

The iterative procedure [Eq. (12)] can be repeated for various neighbors of the ith cell; in order to keep the treatment numerically tractable, we took the drastic step of truncating the interaction potential at second neighbors.

The procedure was then iterated until a prescribed accuracy was achieved. The number of iterations ranged between a few tens and a few hundreds, depending on the number of factors, but mainly on the kernel $V(ij)$. Calculations were carried out using $M = 800$, corresponding to 800^2 points for a Monte Carlo integration of comparable accuracy.

IV. PAIR POTENTIAL MODEL

The kernel of integral equations in Eq. (13) is determined by the pair interaction potential; for two arbitrary molecules (i) and (j), let us first define

$$\mathbf{q}_{ij} = \mathbf{q}_i - \mathbf{q}_j, \quad q_{ij} = |\mathbf{q}_{ij}|, \quad \mathbf{r}_{ij} = \mathbf{q}_{ij}/q_{ij}.$$

The pair potential was chosen to be the sum of a Gay-Berne (GB) [1] and dipole-dipole interaction

$$\Phi(ij) = \Phi_{GB}(ij) + \Phi_{dd}(ij).$$

The GB term has the form [1]

$$\Phi_{GB}(ij) = 4\epsilon_0\epsilon\left[\left(\frac{\sigma_0}{q_{ij}-\sigma+\sigma_0}\right)^{12} - \left(\frac{\sigma_0}{q_{ij}-\sigma+\sigma_0}\right)^{6}\right], \qquad (15)$$

where $\sigma = \sigma(\mathbf{r}_{ij},\mathbf{e}_i,\mathbf{e}_j)$ and $\epsilon = \epsilon(\mathbf{r}_{ij},\mathbf{e}_i,\mathbf{e}_j)$ depend on mutual orientations but not on the distance between centers of mass, and their expressions can be found in Ref. [1], Eqs. (3), (4), (8), (9), and (10). σ depends on the molecular elongation (or length-to-breadth ratio) γ (denoted by $\sigma_\parallel/\sigma_\perp$ in Ref. [1]), whereas ϵ depends on both γ and another parameter, which can be used to adjust the ratio between end-to-end and side-by-side well depths, denoted by ϵ_l/ϵ_s. In our calculations, the parameters μ and ν of Ref. [1] have been fixed to the values 1 and 2, respectively. The dipolar interaction is defined by

$$\Phi_{dd}(ij) = \frac{\Delta^2}{q_{ij}^3}\{\mathbf{e}_i \cdot \mathbf{e}_j - 3(\mathbf{r}_{ij} \cdot \mathbf{e}_i)(\mathbf{r}_{ij} \cdot \mathbf{e}_j)\}, \qquad (16)$$

where Δ is the common magnitude of molecular dipole moments; we are considering here central dipoles along molecular symmetry axes. As pointed out in the preceding section, the interaction was truncated at second neighbors.

V. FORMULAS FOR THE FRANK ELASTIC CONSTANTS

Within the framework of the theory in Ref. [14], based in turn on a density-functional approach, one can write a formally exact expression for the Frank elastic constants, i.e.,

$$\frac{K_{11}}{K} = 1 + \lambda(5-9z), \qquad (17)$$

$$\frac{K_{22}}{K} = 1 - \lambda(1+3z), \qquad (18)$$

$$\frac{K_{33}}{K} = 1 - 4\lambda(1-3z), \qquad (19)$$

where

$$z = \frac{\bar{P}_4 - \bar{P}_6}{\bar{P}_2 - \bar{P}_4}, \quad \lambda = \frac{\omega^2-1}{4(\omega^2+2)}, \qquad (20)$$

$$K = \frac{1}{3}(K_{11}+K_{22}+K_{33}) = \frac{1}{3}L(3\bar{P}_2-1)^2(\bar{P}_2-\bar{P}_4)\frac{3-\omega}{2\omega}, \qquad (21)$$

$$\omega = \frac{\gamma^2 - 1}{\gamma^2 + 1}, \quad L = 3M_4 b^2 \rho^2 \sigma_0^5 \pi \omega^3 \theta \frac{1 + \frac{1}{14}\omega^2}{(1 - \omega^2)^2},$$

$$\text{(22)}$$

$$b = 4\pi\sigma_0^2 \rho \omega^2 M_2 \frac{1 + \frac{3}{14}\omega^2}{3(1 - \omega)};$$

here $M_{2m} = -\int_0^\infty dy\, C(y) y^{2m}$, $m = 1,2$ are radial integrals over the DCF.

Order parameters can be expressed in terms of the function $\psi_i(i)$ as

$$\bar{P}_{2L} = \langle P_{2L}(\cos\theta_i) \rangle_i = \int d(i) F_i(i) P_{2L}(\cos\theta_i), \quad \text{(23)}$$

where θ_i denotes the polar angle, i.e., the angle between the long axis of the molecule and the director, taken to coincide with the cell z axis.

There exists another density-functional approach [15] connecting elastic properties of the nematic with structural quantities such as the one-particle distribution function and the DCF, both of an aligned nematic. Based on the Onsager approximation for the DCF, i.e.,

$$C(\mathbf{q}_{ij}, \mathbf{e}_i, \mathbf{e}_j) = \exp\{-\beta\Phi(\mathbf{q}_{ij}, \mathbf{e}_i, \mathbf{e}_j)\} - 1, \quad \text{(24)}$$

the Frank elastic constants are expressed by

$$\frac{K_{11}}{K} = 1 + \lambda_1 - 3\lambda_2 z_1, \quad \text{(25)}$$

$$\frac{K_{22}}{K} = 1 - 2\lambda_1 - \lambda_2 z_1, \quad \text{(26)}$$

$$\frac{K_{33}}{K} = 1 + \lambda_1 + 4\lambda_2 z_1, \quad \text{(27)}$$

where

$$z_1 = \frac{\bar{P}_4}{\bar{P}_2}, \quad \lambda_1 = \frac{2R^2 - 2}{7R^2 + 20}, \quad \lambda_2 = \frac{27}{16}\frac{R^2 - 1}{7R^2 + 20}, \quad R = \gamma - 1.$$

$$\text{(28)}$$

In the framework of the theory in Ref. [14], Nemtsov took a different approximation for the DCF, $C(\mathbf{q}_{ij}, \mathbf{e}_i, \mathbf{e}_j) = C(q_{ij}/\sigma)$, where σ is the size parameter, which depends on molecular orientations, and is given by Eqs. (8)–(10) of Ref. [1]; this turned out to work slightly better than Onsager's approach.

Another remark on the level approximations involved is appropriate: one can calculate the set of order parameters in the framework of a statistical-mechanical theory which accounts for intercell pair correlations, based, for example, on the concept of average force potentials. However, the DCF used in the expressions for the elastic constants [(17)–(19) and (24)–(26)] has been calculated in the framework of the mean-field theory [see also Eq. (35) of Ref. [6]], where the repulsive interaction has the form of a hard-core potential with an angle-dependent size parameter σ, and the attractive part is treated to first order in perturbation theory. In other words, one can calculate the set of order parameters at one
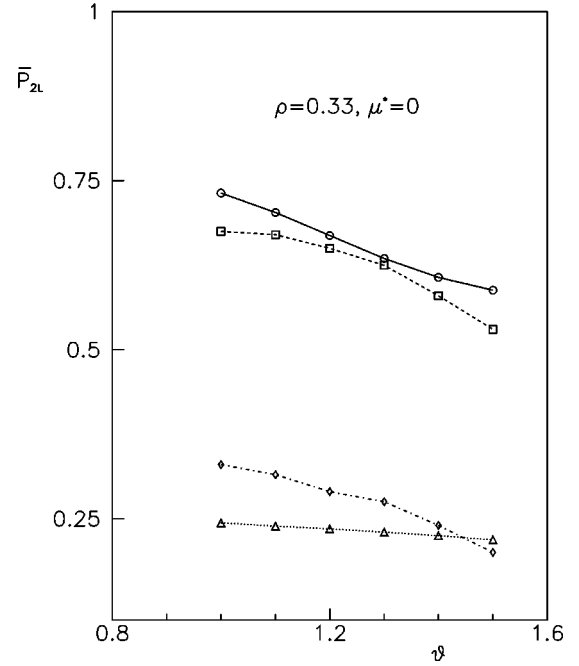

FIG. 1. Temperature dependence of orientational order parameters $\bar{P}_{2L}$ for the pure GB model, at constant density. Circles, $\bar{P}_2$; triangles, $\bar{P}_4$ in the framework of the present theory; squares and diamonds refer to $\bar{P}_2$ and $\bar{P}_4$, respectively, as estimated by molecular-dynamics simulation [7] at the same density.

level of rigor, but then use a lower one in the final expressions for the elastic constants. Here we attempt to take into account the influence of intercell pair correlations on the elastic constants, in the framework of average force potentials, by calculating the ratios K_{ii}/K and avoiding explicit calculation of the DCF.

VI. NUMERICAL RESULTS

Our calculations have been performed for temperatures and densities, corresponding to the nematic phase. Reduced units have been used for density ($\rho = \sigma_0^3/v$), temperature ($\beta^{-1} = \theta = k_B T/\epsilon_0$), dipole moment [$\mu^* = \Delta/(\sigma_0^3 \epsilon_0)^{1/2}$], and anisotropy parameter γ, for which the value $\gamma = 3$ was chosen.

Figure 1 reports the temperature dependence of order parameters $\bar{P}_{2L}$ at fixed density $\rho = 0.33$, and shows a good agreement with the corresponding simulation results from Ref. [7]; Fig. 2 shows the density dependence of the nematic order parameters $\bar{P}_{2L}$ at fixed temperature $\theta = 1$, for both polar and nonpolar models; the density range ($0.27 \leq \rho \leq 0.33$) corresponds to the nematic range of the GB fluid. As expected, orientational order is found to increase with increasing density. Figure 3 shows the temperature dependence of the elastic constants K_{ii}/K, at fixed density $\rho = 0.33$, calculated using the different approaches mentioned above and compared with results of molecular-dynamics simulations at the same thermodynamics condition [7]; on the whole, the difference between the reseults obtained by the two theoretical treatments is roughly independent of temperature. Results of calculations for splay deformation K_{11}/K (black symbols: circles, squares, triangles) show the best agreement
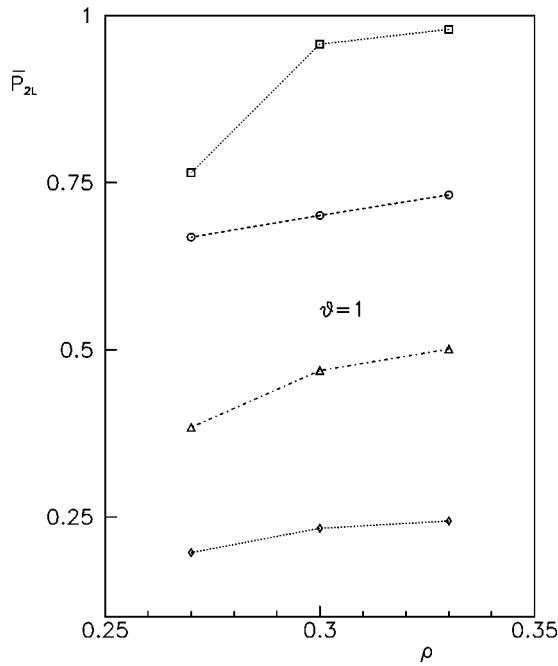
FIG. 2. Density dependence of orientational order parameters $\bar{P}_{2L}$ at constant temperature, and for different values of the reduced dipole moment. Circles, $\bar{P}_2$ for $\mu^*=0$; diamonds, $\bar{P}_4$ for $\mu^*=0$; squares and triangles refer to $\bar{P}_2$ and $\bar{P}_4$, respectively, and $\mu^* = 2$.
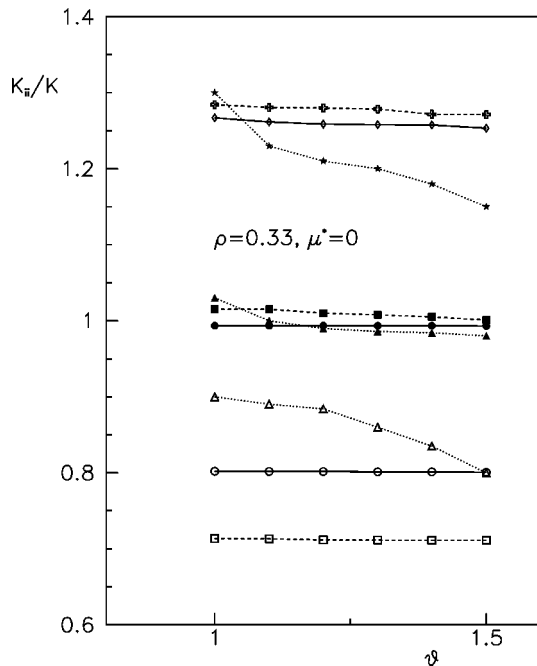

FIG. 3. Temperature dependence of the ratio K_{ii}/K at constant density. Black circles, values of K_{11}/K calculated by means of Eq. (17); black squares, the same values based on Eq. (24); black triangles, values of splay deformations recalculated from Fig. 6 in Ref. [7]. Empty circles, values of K_{22}/K calculated by means of Eq. (18); empty squares, the same values based on Eq. (25); empty triangles, values of twist deformation recalculated from Fig. 6 in Ref. [7]; stars, values of K_{33}/K calculated by means of Eq. (19); crosses, the same value based on Eq. (26); diamonds, values of bend deformation recalculated from Fig. 6 in Ref. [7].

between the two theoretical approaches as well as with simulation results: results of both calculations for twist and bend deformations show more pronounced differences from the results obtained by the two theoretical approaches, as well as with simulation results: in Fig. 3 the disagreement with simulation results for K_{22}/K increases with lowering temperature, whereas for bend deformation K_{33}/K the same differences increase with increasing temperature.

The present results show a pronounced increase of $\bar{P}_2$ with increasing dipolar contribution; this is in qualitative agreement with simulation results obtained by various authors [10–12], showing that a strong dipolar contribution can even favor smectic ordering.

In a few cases we examined the effect of different truncation radii; for example, when $\rho=0.33$, $\theta=1$, and $\mu^*=1$, we found a change in $\bar{P}_2$ from 0.954 (nearest neighbors) to 0.9695 (second neighbors); for the same values of ρ and θ, but $\mu^*=2$, $\bar{P}_2$ similarly changed from 0.9695 to 0.9806. Results quoted in the following were obtained by taking into account first and second neighbors only.

The most rigorous test of the theory would be a comparison with the Monte Carlo simulations for the same pair potential. Such computer simulation data for OP $\bar{P}_2$ have been reported [10] at fixed temperature $\theta=1.2$, density $\rho=0.3$, and dipolar moment $\mu^*=2.0$. We found a change in $\bar{P}_2$ from 0.963 (in our calculations) to 0.97 (in Ref. [10]).

Figure 4 shows the effect of dipolar interactions on order parameters $\bar{P}_{2L}$, at fixed density $\rho=0.33$, and for two temperatures; Fig. 2 shows the influence of dipolar interaction on order parameters $\bar{P}_{2L}$, for the number of densities, at fixed temperature $\theta=1.0$; they both point to a significant
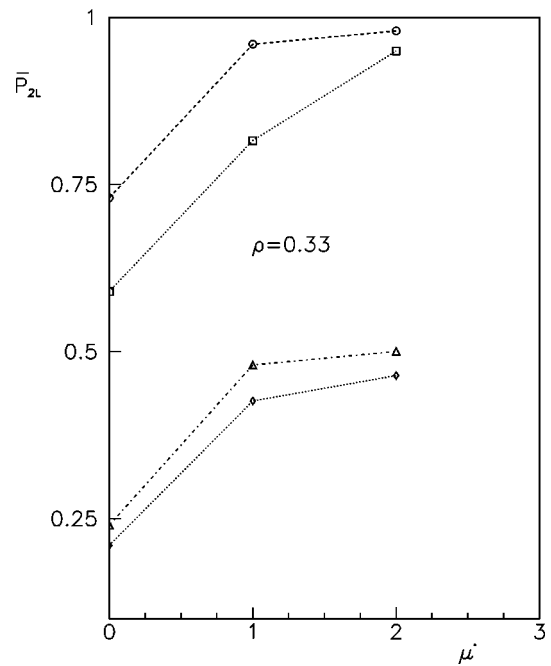

FIG. 4. Influence of the dipolar interaction on orientational order parameters $\bar{P}_{2L}$ at constant density, and for different temperatures. Circles, $\bar{P}_2$ at $\theta=1$; triangles, $\bar{P}_4$ at the same temperature; squares and diamonds refer to $\bar{P}_2$ and $\bar{P}_4$, respectively, at $\theta=1.5$.
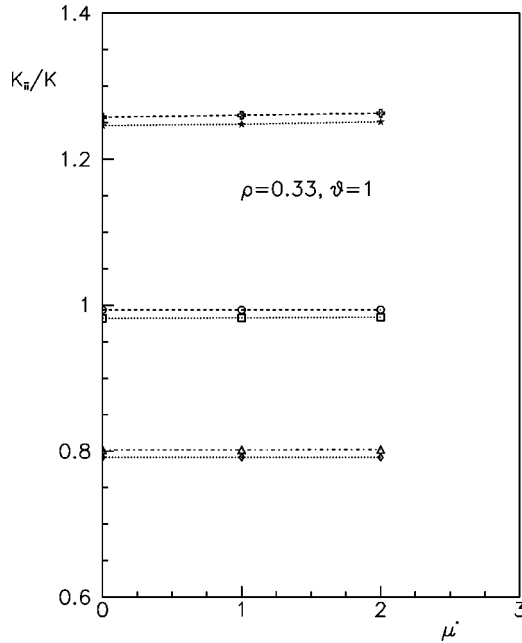
FIG. 5. Influence of the dipolar interaction on the ratios K_{ii}/K, at constant density and constant temeprature. Crosses, K_{33}/K by Eq. (19); stars, K_{33}/K by Eq. (26); circles, K_{11}/K by Eq. (17); squares, K_{11}/K by Eq. (24); triangles, K_{22}/K by Eq. (18); diamonds, K_{22}/K by Eq. (25).

strengthening of orientational order with increasing density and dipole moment.

Finally, Fig. 5 reports μ^* dependences of the ratios K_{ii}/K, at fixed density $\rho=0.33$ and temperature $\theta=1$; Fig. 6 reports their density dependence at fixed temperature ($\theta=1$), at two different values of μ^*. Notice that individual order parameters exhibit a pronounced dependence on μ^*, but the ratios of the elastic constants depend on the order parameters via their combinations z and z_1 [see Eqs. (17)–(26)], whose μ^* dependence is rather weaker. On the other hand, a strong density dependence of the individual elastic constants K_{ii} should be expected, since $K_{ii}\sim\rho^2$ (see the equations in Sec. V).

VII. CONCLUSIONS

In this paper, a statistical-mechanical theory based upon the method of conditional distribution functions has been applied to calculate structural properties and Frank elastic constants for a system consisting of cylindrically symmetric particles interacting via a Gay-Berne pair potential, also supplemented by a dipolar term. Calculations of the elastic constants of the purely Gay-Berne model have been carried out on a simple-cubic system, and for a range of temperature and densities corresponding to the nematic phase, as in the phase diagram calculated by de Miguel and Rull [26]. Two analytical theories expressing the elastic constants in terms of DCF have been tested [14,15], and a good agreement has been found between their predictions, as well as with results obtained by molecular-dynamics simulation [7], via expansion of the DCF on the basis of S functions.

In addition to the pure GB model, we have also investigated the effect of dipolar interaction although in a more approximate way, since a proper treatment of its long-range
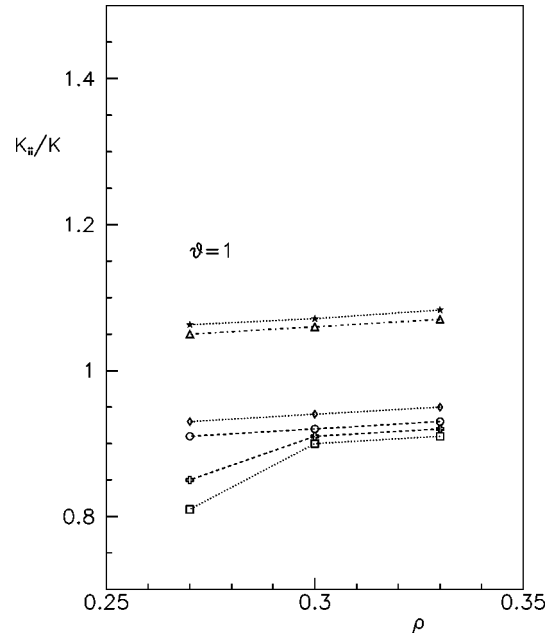

FIG. 6. Density dependence of the ratios K_{ii}/K, at constant temperature, and for two values $\mu^*=0$ and $\mu^*=2$. Stars and triangles indicate ratios K_{33}/K calculated by means of Eq. (19) for $\mu^*=0$ and $\mu^*=2$, respectively. Diamonds and circles indicate ratios K_{11}/K calculated by means of Eq. (17) for $\mu^*=0$ $\mu^*=2$, respectively. Crosses and squares indicate ratios K_{22}/K calculated by means of Eq. (18) for $\mu^*=0$ and $\mu^*=2$, respectively.

character would become computationally prohibitive.

On the basis of these calculations, it is concluded that the elastic constants are affected in a more pronounced way by changes in the thermodynamic state than by dipolar interactions. We also wish to comment on the approximations involved in this and similar treatments. At the first level, some kind of approximation is needed in order to calculate order parameters, which may or may not involve neglecting short-range pair correlations.

At the second level, some simplified version of the DCF has to be used, and this often means neglecting short-range pair correlations, even if taken into account at the previous one; the procedure is expected to yield better estimates of ratios between elastic constants than of their individual values.

APPENDIX: SOBOL'S METHOD [24]

The LP_τ generator has been organized as follows: one initially new sequence $W_j^{(l)}=r_j^{(l)}2^{-1}$, where entries $r_j^{(l)}$ were takes from Table 1 of Ref. [24], and each $W_j^{(l)}$ were expressed as finite binary fraction. If the binary representation of an arbitrary integer i is $e_m\cdots e_2e_1$, then the jth compo-

nent of the point P_α is given by $P_\alpha^j = e_1 W_j^{(1)} \star e_2 W_j^{(2)} \star \cdots \star e_m W_j^{(m)}$, where $\star$ denotes addition modulo 2 in each binary place, and $j = 1, \ldots, n$. We used the relatively slow arithmetic program for creation of the LP_τ sequence: the effort to generate an n-dimensional point P_α is proportional to $(\log_2 \alpha)^2 n$.

Coordinates P_α in Eq. (13) were chosen such that $\psi_i^{[11]}(P_\alpha)$ could be calculated at points forming the same stationary LP_τ sequence as used in the evaluation of integrals with the initial approximation $\psi_i^{[0]}(P_\alpha)$. In other words, the grid points are generated once and for all; a more detailed discussion of LP_τ sequences can be found in Ref. [25].

[1] J. G. Gay and B. J. Berne, J. Chem. Phys. **74**, 3316 (1981).

[2] E. de Miguel, L. F. Rull, M. K. Chalam, and K. E. Gubbins, Mol. Phys. **74**, 405 (1991).

[3] G. R. Luckhurst, R. A. Stephens, and R. W. Phippen, Liq. Cryst. **8**, 451 (1990); G. R. Luckhurst and P. S. J. Simmonds, Mol. Phys. **80**, 233 (1993).

[4] J. T. Brown, M. P. Allen, E. Martín del Río, and E. de Miguel, Phys. Rev. E **57**, 6685 (1998).

[5] S. Sarman, J. Chem. Phys. **105**, 4211 (1996); Physica A **240**, 160 (1997).

[6] P. I. C. Teixeira, V. M. Pergamenshchik, and T. J. Sluckin, Mol. Phys. **80**, 1339 (1993).

[7] J. Stelzer, L. Longa, and H. R. Trebin, J. Chem. Phys. **103**, 3098 (1995).

[8] J. Stelzer, M. A. Bates, L. Longa, and G. R. Luckhurst, J. Chem. Phys. **107**, 7483 (1997).

[9] G. Vertogen and W. H. de Jeu, *Thermotropic Liquid Crystals: Fundamentals* (Springer, Berlin, 1988).

[10] K. Satoh, S. Mita, and S. Kondo, Liq. Cryst. **20**, 757 (1996); Chem. Phys. Lett. **255**, 99 (1996).

[11] R. Berardi, S. Orlandi, and C. Zannoni, Chem. Phys. Lett. **261**, 357 (1996); J. Chem. Soc., Faraday Trans. **83**, 1493 (1997).

[12] M. Houssa, A. Oualid, and L. F. Rull, Mol. Phys. **94**, 439 (1998).

[13] A. V. Zakharov, Phys. Rev. E **51**, 5880 (1995).

[14] V. B. Nemtsov, Theor. Appl. Mech. (Minsk) **13**, 16 (1987); A. V. Zakharov, Physica A **175**, 327 (1991).

[15] A. Poniewierski and J. Stecki, Mol. Phys. **38**, 1931 (1978).

[16] L. A. Rott, *Statistical Theory of Molecular Systems* (Nauka, Moscow, 1978).

[17] M. W. Matsen and D. E. Sullivan, Phys. Rev. A **41**, 2021 (1990).

[18] J. A. Barker, J. Chem. Phys. **63**, 632 (1975).

[19] D. M. Burley, in *Phase Transitions and Critical Phenoman*, edited by C. Domb and M. S. Green (Academic Press, London, 1972), Vol. 2, Chap. 9, pp. 329–374.

[20] C. Chiccoli, P. Pasini, F. Biscarini, and C. Zannoni, Mol. Phys. **65**, 1505 (1988).

[21] P. Biscarini, C. Zannoni, C. Chiccoli, and P. Pasini, Mol. Phys. **73**, 439 (1991).

[22] N. V. Marchenko, Dokl. Akad. Nauk SSSR **137**, 515 (1961).

[23] E. T. Brook-Levinson, A. V. Zakharov, and L. A. Rott, Dokl. Akad. Nauk BSSR **30**, 917 (1986).

[24] I. M. Sobol, SIAM (Soc. Ind. Appl. Math.) J. Numer. Anal. **16**, 790 (1979).

[25] N. M. Korobov, Dokl. Akad. Nauk SSSR **115**, 1062 (1957).

[26] E. de Miguel and L. F. Rull, Mol. Phys. **74**, 405 (1991).